Prethermalization and dynamic phase transition in an isolated trapped ion spin chain

Article *in* New Journal of Physics · November 2013

DOI: 10.1088/1367-2630/15/11/113051

Prethermalization and dynamical transition in an isolated trapped ion spin chain

Zhe-Xuan Gong[1, 2, *] and L. -M. Duan[1, 2]

[1] *Department of Physics, University of Michigan, Ann Arbor, Michigan 48109, USA*
[2] *Center for Quantum Information, IIIS, Tsinghua University, Beijing, 100084, P. R. China*

We propose an experimental scheme to observe prethermalization and dynamical transition in one-dimensional XY spin chain with long range interaction and inhomogeneous lattice spacing, which can be readily implemented with the recently developed trapped-ion quantum simulator. Local physical observables are found to relax to prethermal values at intermediate time scale, followed by complete relaxation to thermal values at much longer time. The physical origin of prethermalization is explained by spotting a non-trivial structure in lower half of the energy spectrum. The dynamical behavior of the system is shown to cross difference phases when the interaction range is continuously tuned, indicating the existence of dynamical phase transition.

The dynamical properties of isolated quantum many-body systems have been under intense interest in recent years [1, 2]. On the theory side, the research has been centered on whether and how an isolated quantum system approaches thermal equilibrium. While certain observables are found to relax to equilibrium in some large systems [3–7], it remains unclear on what conditions and time scale equilibration occurs in generic systems [8–11]. On the experimental side, recent progress with cold atoms [12–14] and trapped ions [15–20] has made it possible to simulate well controlled simple models, such as one-dimensional (1D) Bose gas and transverse field Ising model. These quantum systems can be well isolated from the environmental bath and have long coherence time, while their physical properties can be measured at individual atomic level, providing an unprecedented opportunity for studying non-equilibrium dynamics in closed interacting systems.

A particularly intriguing phenomenon in this context is called *prethermalization* [21], which has been shown to emerge in various theoretical setups [22–24], and experimentally observed in cold atomic gas [14]. The emergence of prethermalization is characterized by establishment of quasi-stationary state at intermediate time scale, and followed by relaxation to stationary state at much longer time scale (thermalization). Physical origin of prethermalization, however, is still elusive, and is primarily speculated to be related to quasi-integrability of the model [14, 23].

In this paper, we propose a new experimental scheme for observing and studying prethermalization and related dynamical transition in a XY spin model, which can be implemented with the current trapped-ion quantum simulator [19]. Our model features long range spin-spin interaction with inhomogeneous lattice spacing, and unlike many other systems, the prethermalization can occur already for as few as a dozen of spins, allowing for its observation in current experimental systems. The prethermalization shown up in this system has a quite different mechanism and we find that a non-trivial structure in the energy spectrum resulting from long-range interaction and inhomogeneous lattice is responsible for the occurrence of prethermalization in our model. In addition, by tuning the range of interaction with an experimental knob, we find the dynamical behavior of system exhibits three different phases: thermalization only, prethermalization followed by thermalization, and prethermalization only. The transition between different phases becomes sharper and sharper with increased number of spins, hinting the existence of dynamical phase transitions [25].

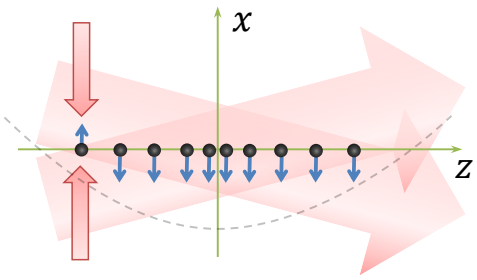

Figure 1: Schematic of the proposed experimental setup: A chain of N ions are trapped along the z direction in a 1D harmonic linear Paul trap. The global Raman beams generate spin-dependent force along x direction, resulting in effective Ising-type interaction. To induce dynamics, a focused laser beam is applied on one end of the ion chain to selectively flip only the first spin.

Model and its dynamics Our spin model is based on the experimental system of a chain of ions confined in a linear Paul trap (Fig. 1). Through proper configuration of Raman beams, the optical dipole force can generate an effective transverse field Ising model [16, 17, 26]:

$$H = \sum_{i<j}^{N} J_{i,j}\sigma_i^x\sigma_j^x + B\sum_{i=1}^{N}\sigma_i^z, \tag{1}$$

where σ_i is the spin-1/2 Pauli matrix for the i^{th} ion qubit.

*Electronic address: gzx@umich.edu

The interaction coefficient J_{ij} in Eq. (1) is given by

$$J_{i,j} = \Omega^2 \sum_{m=1}^{N} \frac{\eta_{i,m}\eta_{j,m}\omega_m}{\mu^2 - \omega_m^2},$$

where μ is the Raman beatnote frequency, Ω is the effective Rabi frequency, which is assumed to be uniform on all the ions, $\{\omega_m\}$ are the phonon mode frequencies of ions in x direction, and $\eta_{i,m}$ are the Lamb-Dicke parameters measuring the coupling between the ith ion and the mth phonon mode. We are interested in the region where $B \gg \max\{J_{ij}\}$. In this limit, the $\sigma_i^+\sigma_j^+$ and $\sigma_i^-\sigma_j^-$ terms in Eq. 1 will be energetically forbidden, and we end up with the XY Hamiltonian:

$$H \approx H_{XY} = \sum_{i<j} 2J_{i,j}(\sigma_i^+\sigma_j^- + h.c.) + B\sum_i \sigma_i^z \qquad (2)$$

A unique feature of the Hamiltonian (1 & 2) realized with the ion system is that the interaction characterized by J_{ij} is long-ranged and the range of interaction can be readily tuned by changing the beatnote frequency μ. In particular, in a range of μ, J_{ij} can be roughly approximated by an power-law decay with $J_{ij} \sim |i-j|^{-\alpha}$, where α varies from 0 to 3 when we tune μ[19]. In our following analysis, for a given μ, we fit the coefficient J_{ij} with $J_{ij} \sim |i-j|^{-\alpha}$ and use the fitting parameter α as an indicator of the range of iteration.

To study dynamics of the model Hamiltonian (2), we first initialize all the spins through optical pumping to the spin down state with $\sigma_i^z = -1$, which is an eigenstate of H_{XY} and hence stationary. We then use a focused laser beam to flip the first spin (left end ion) to $\sigma_i^z = 1$ (see Fig. 1). The starting state $|\psi(0)\rangle = |\uparrow\downarrow\downarrow\cdots\downarrow\rangle$ is no longer an eigenstate of H_{XY} and subject to dynamics with $|\psi(t)\rangle = e^{iH_{XY}t/\hbar}|\psi(0)\rangle$. We consider time evolution of local observables $\langle\sigma_i^z(t)\}$ and their correlations $\langle\sigma_i^z(t)\sigma_j^z(t)\rangle$ which can be directly measured in experiments. For convenience of description of the dynamics, we introduce the operator

$$C = \sum_{i=1}^{N} f_i \frac{\sigma_i^z + 1}{2}$$

where the coefficient $f_i \equiv (i - \frac{N+1}{2})/(N-1)$ is equally distributed between $[-1, 1]$ from $i = 1$ to $i = N$. The expectation value of C varies between $[-1, 1]$ and physically measures the relative position of the spin excitation. It's easy to check that $\langle\psi(0)|C|\psi(0)\rangle = -1$,meaning the spin excitation is at the left edge of the chain. For any state with spatial inversion symmetry around the center of the chain, $\langle C\rangle = 0$.

Prethermalization and dynamical transition: To find out the dynamical behavior, we first perform numerical calculation with an $N = 16$ ion chain, which corresponds to the size of the current experimental platform for ion quantum simulator [19]. As shown in Fig. 2, we pick up two parameter settings with the corresponding fitting

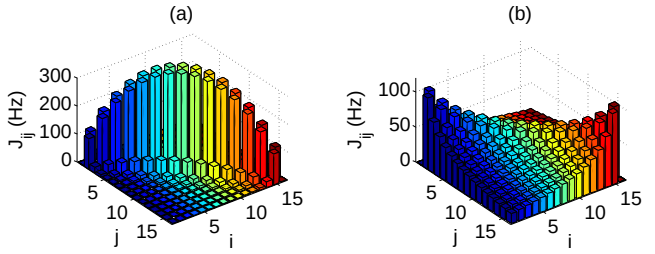

Figure 2: (a) Distribution of J_{ij} for short range interaction with the beatnote frequency set at $\mu = 5.2$ MHz, the trap frequency in z direction $\omega_z = 100$ KHz, and $\eta_x\Omega = 40$ KHz. The corresponding fitting parameter $\alpha \approx 2.6$ in this case. (b) Distribution of J_{ij} for long range interaction with $\mu = 5.02$ MHz, $\omega_z = 600$KHz, $\eta_x\Omega = 3.9$KHz, and the corresponding fitting parameter $\alpha \approx 0.52$. In both cases we have trap frequency in x direction $\omega_x = 5$ MHz and average interaction strength $J_0 = \sum_{i\neq j} J_{ij}/N^2 = 20$ Hz.

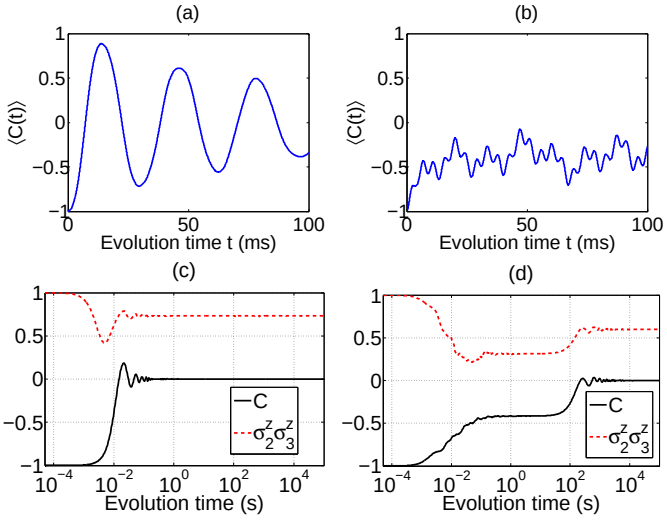

Figure 3: (a-b) Short time dynamics of σ_i^z and C for short-range (a) and long-range (b) interaction. (c-d) Long time dynamics of time-averaged C and $\sigma_i^z\sigma_j^z$ for (c) short-range and (d) long-range interaction. The parameters for short-range and long-range interaction are given by Fig. 2

parameter $\alpha \approx 2.6$ and $\alpha \approx 0.52$, which represent respectively short-range and long-range interaction. The distributions of the exact coupling coefficients J_{ij} are shown in Fig. 2 for these two cases.

For these choices of parameters, the short time dynamics with $t \in [0, 2/J_0]$ for all $\langle\sigma_i^z\rangle$ and $\langle C\rangle$ are shown in Fig. 3. In the short-range interaction case, one observes that the spin excitation, initially located at the left edge of the chain, almost coherently travels to the other side and oscillates back and forth with relatively small dispersion. In contrast, the spin excitation diffuses to the rest of the chain in the long-range interaction case and somehow get locked before it reaches the middle of the chain (with $\langle C\rangle \approx -0.4$).

To better show the long time dynamics, we use the

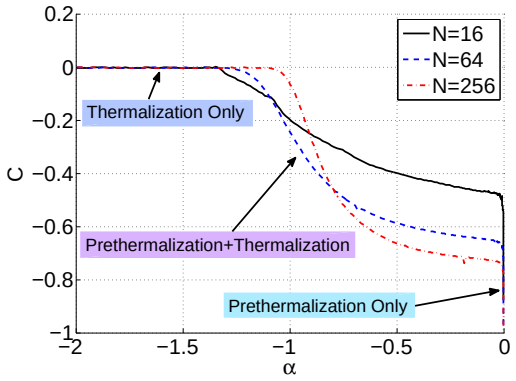

Figure 4: A dynamical "phase diagram" with regard to the interaction range characterized by the fitting parameter α. The $N = 16$ case uses the parameters specified in Fig. 1 and $N = 64, 256$ cases use the same parameters except that ω_z is scaled down by $\omega_z \propto \sqrt{\ln N}/N$ to maintain chain stability.

finite-time-averaged quantity $\overline{A(t)}$, defined as $\overline{A(t)} \equiv \frac{1}{t}\int_0^t \langle A(\tau)\rangle d\tau$ for the observable A [27, 28]. This will average out temporal fluctuations on short time scale (the following dynamical behaviors are qualitatively the same even without performing any time averaging). The long time dynamics is shown in Fig. 3(c-d). In the short-range interaction case, the spin excitation position C, as well as the spin correlation $\sigma_i^z\sigma_j^z$, relax to the stationary values at around $T_0 \approx 10/J_0 = 500ms$. In the long-range interaction case, observables first reach quasi-stationary (prethermal) values at time scale T_0, and further relax to the stationary (thermal) values at much longer time scale ($10^4 T_0$). The emergence of prethermalization is manifested in the long-range interaction case by a nonzero value of $\overline{C}$ at intermediate time scale T_0. We can use $\overline{C}$ as an order parameter to characterize different dynamical behaviors. By continuously tuning the effective interaction range (indicated by the fitting parameterα) with the beatnote frequency μ, we find that (see Fig. 4) prethermalization only takes place when α is smaller than a critical value ($\alpha_C \approx 1.3$ for $N = 16$). For larger system size, the prethermalization-thermalization transition still occurs, but α_C becomes smaller and the transition becomes sharper. For the particular case $\alpha = 0$, the system has uniform coupling and its dynamics can be solved exactly. The exact solution shows that the system stays in the prethermal state forever with $\overline{C} = \frac{2}{N} - 1$.

Mechanism of prethermalization and dynamical transition . We now give a physical explanation to why prethermalization and different dynamical behaviors occur in this model. The distinctive short time dynamics of $\langle\sigma_i^z(t)\rangle$ (Fig. 3a,b) can be explained by examining the energy spectrum of H_{XY} in the single spin excitation subspace (shown in Fig. 5a). In the short-range interaction case, the energy spectrum is close to linear. This is because H_{XY} can be roughly approximated with only neighboring interaction, which is then identical to a tight-binding fermionic model

$$H_{tb} = 2\sum_i (J_{i,i+1}c_i^\dagger c_{i+1} + Bc_i^\dagger c_i)$$

and shows "quantum mirror" behavior [29, 30], resulting in a near dispersion-free spin wave propagation until nonlinearity sets in. On the other hand, the energy spectrum for the long range interaction case is highly non-linear, so the dynamics of spin excitation is strongly dispersive.

The cause for existence of prethermal stage in the long time dynamics, however, is much more complicated. Naively, the spin flip-flop matrix J_{ij} varies smoothly among sites for any $\alpha \in (0, 3)$, so the spin excitation should continuously diffuse from one end of the chain to the whole chain, and is not expected to get trapped somewhere in the middle for a long time. The two stage dynamics indicates that there are two different time scales weaved in the Hamiltonian, which is not at all obvious by looking at J_{ij}. We note, however, that the time dynamics of any physical observable is simply given by

$$\langle A(t)\rangle = \sum_{m,n} \rho_{mn}(0)A_{nm}e^{i(E_m-E_n)t/\hbar},$$

where $\rho_{mn}(0)$ is the initial state's density matrix element in energy basis. So different time scales of dynamics can be unraveled through mapping of eigenenergy differences $\{E_m - E_n\}$, as done in Fig. 5. In the short-range interaction case (Fig. 5b), all $\{E_m - E_n\}$ are continuously distributed from J_0 to $100J_0$, so a single-stage relaxation is expected after $T \sim T_0 = 10/J_0$. In the long-range interaction case (Fig. 5c), most $\{E_m - E_n\}$ still fall into the range of $1-100J_0$, but there is a striking separate branch gaped at much lower rate ($\sim 10^{-6}J_0$). This branch actually corresponds to near-degenerate pairs ($\{E_{2k}-E_{2k-1}\}$) of eigenenergy (Fig. 5a) that make up the first half energy spectrum, and the number of these pairs scale up with system size N. The appearance of near-degenerate pairs $\{E_{2k} - E_{2k-1}\}$) in eigenspectrum of our model seems to be due to a combined effect of long-range interaction and inhomogeneous lattice spacing. If we put the ions into a ring (or flat-bottomed) trap so that the ions are equally spaced, we find that there is no separate branch in $\{E_m - E_n\}$ plot (figure not shown) and hence no prethermalization behavior even with the same long-range interaction.

Figure 5d shows that the thermal values can be well predicted by the diagonal ensemble (DE), defined as

$$\rho_{DE} = \rho_{mn}(0)\delta_{mn},$$

In large N limit, under certain conditions prescribed as *eigenstate thermalization hypothesis* [3–5], the diagonal ensemble prediction will match the canonical ensemble for thermalized state in classical statistical physics.

As prethermalization is due to a different scale of eigenenergy difference in the Hamiltonian, to predict the

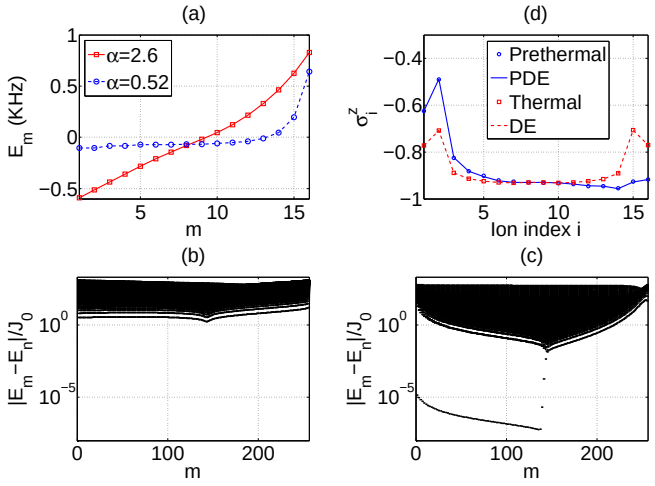

Figure 5: (a) Energy spectrum in the single spin excitation subspace for $N = 16$ spins with short and long range interaction. (b-c) Scatter plot of eigenenergy differences $\{E_m - E_n\}$ for $N = 256$ spins with (b) short range interaction ($\alpha = 2.4$) and (c) long range interaction ($\alpha = 0.74$). (d) Comparison of prethermal values of $\overline{\sigma_i^z}$ (blue circle, taken at $t = T_0 = 500ms$) with PDE prediction (blue solid line) and thermal values (red square, taken at $t = 5\times10^3 s$) with DE prediction (red dashed line) based on long range interaction pattern J_{ij} shown in Fig. 2b. See in the text for the definition of PDE and DE.

prethermal values here, we can define the *partial diagonal ensemble* (PDE):

$$\rho_{PDE} = \begin{cases} \rho_{mn}(0)\delta_{mn} & |\nu_m - \nu_n| \gtrsim 1/T_0 \\ \rho_{mn}(0) & |\nu_m - \nu_n| \ll 1/T_0 \end{cases}$$

where $\{\nu_m\}$ are the eigenenergies. We find that the PDE can well predict prethermal values of local observables $\overline{\sigma_i^z}$, as shown in Fig. 5d. Roughly speaking, the prethermalization time scale is determined by the average level spacing ($\sim 10/J_0$), and the thermalization time scale is determined by the minimum level spacing ($\sim 10^4/J_0$ as in Fig. 5d).

The dynamical transition can be associated with breaking of the lattice inversion (parity) symmetry, reminiscent of symmetry breaking in equilibrium phase transitions. Our Hamiltonian H_{XY} is symmetric under the space inversion around $z = 0$ (Fig. 1), but we start from an initial state that does not have this symmetry. The thermal state, with no memory of initial state, is described by the diagonal ensemble ρ_{DE} and restores this symmetry as $\overline{C} = 0$. However, the prethermal state does not restore the Hamiltonian symmetry due to its non-zero $\overline{C}$ value, which indicates that some "memory" of initial state is preserved in prethermal state. The intermediate time scale T_0 for observation of the prethermal state gives a microscopic interpretation why this state can break the parity symmetry: one cannot distinguish the near-degenerate pairs of eigenstates in the energy spectrum, so linear combinations within each pair are allowed. Since the two eigenstates of the pair have either even or odd parity, their linear combinations can break the parity symmetry. The dynamical phase diagram shown in Fig. 4) also has the hint of two non-analytic points: one is where $\overline{C}$ becomes non-zero, representing the appearance of prethermalization, and the other is where $\overline{C}$ approaches $\frac{2}{N} - 1$ ($\alpha \to 0$), representing the disappearance of thermalization.

Discussion of experimental detection: The transverse field Ising Hamiltonian Eq. 1 has already been experimentally simulated in Ref. [19] for $N = 16$ ions, with demonstrated highly-efficient in-situ measurement of spin polarization (σ_i^z) and spin correlation ($\sigma_i^z\sigma_j^z$). The XY Hamiltonian (Eq. 2) can thus be readily obtained by tuning up the effective transverse magnetic field. The non-equilibrium initial state preparation requires focused laser beam, but is relatively easy due to large ion spacing near the ends. The laser power and trap frequencies used for generating interaction pattern J_{ij} as shown in Fig. 2 are within current experimental reach [17, 19]. The observation of prethermalization and the dynamical transition shown in Fig. 3 & 4 only requires the spin decoherence time longer than $T_0 = 10/J_0 = 500ms$, and coherence time up to 2.5s has been experimentally achieved using the hyperfine qubit of Yb^+ ions [31]. But the second stage of thermalization for long-range interaction case will take much longer time and is beyond current experimental reach, similar to the experiment on prethermalization with cold atoms [14].

In summary, we have proposed a novel scheme to observe the peculiar prethermalization phenomenon and dynamical transitions in the experimental system of trapped ion quantum simulator. The required conditions fit well with the current experimental technology. We provide an explanation of the mechanism of prethermalization and dynamical transition in our proposed model, which is connected with some unique feature of this experimental system.

Acknowledgments

We thank C. Monroe, A. Polkovnikov, and A. Gorshkov for helpful discussions. This work was supported by the NBRPC (973 Program) 2011CBA00302, the DARPA OLE program, the IARPA MUSIQC program, and the ARO/AFOSR MURI program.

[1] A. Polkovnikov, K. Sengupta, A. Silva, and M. Vengalattore, Reviews of Modern Physics **83**, 863 (2011).

[2] M. A. Cazalilla and M. Rigol, New Journal of Physics

12, 055006 (2010).
[3] J. M. Deutsch, Physical Review A **43**, 2046 (1991).
[4] M. Srednicki, Physical Review E **50**, 888 (1994).
[5] M. Rigol, V. Dunjko, and M. Olshanii, Nature **452**, 854 (2008).
[6] M. Rigol, V. Dunjko, V. Yurovsky, and M. Olshanii, Physical Review Letters **98**, 050405 (2007).
[7] P. Reimann, Physical Review Letters **101**, 190403 (2008).
[8] L. Masanes, A. J. Roncaglia, and A. Acín, Physical Review E **87**, 032137 (2013).
[9] F. G. S. L. Brandão, P. Ćwikliński, M. Horodecki, P. Horodecki, J. K. Korbicz, and M. Mozrzymas, Physical Review E **86**, 031101 (2012).
[10] P. Reimann and M. Kastner, New Journal of Physics **14**, 043020 (2012).
[11] Z.-X. Gong and L.-M. Duan, arXiv:1109.4696 (2011).
[12] T. Kinoshita, T. Wenger, and D. S. Weiss, Nature **440**, 900 (2006).
[13] S. Trotzky, Y.-A. Chen, A. Flesch, I. P. McCulloch, U. Schollwöck, J. Eisert, and I. Bloch, Nature Physics **8**, 325 (2012).
[14] M. Gring, M. Kuhnert, T. Langen, T. Kitagawa, B. Rauer, M. Schreitl, I. Mazets, D. A. Smith, E. Demler, and J. Schmiedmayer, Science **337**, 1318 (2012).
[15] A. Friedenauer, H. Schmitz, J. T. Glueckert, D. Porras, and T. Schaetz, Nat Phys **4**, 757 (2008).
[16] K. Kim, M.-S. Chang, S. Korenblit, R. Islam, E. E. Edwards, J. K. Freericks, G.-D. Lin, L.-M. Duan, and C. Monroe, Nature **465**, 590 (2010).
[17] R. Islam, E. Edwards, K. Kim, S. Korenblit, C. Noh, H. Carmichael, G.-D. Lin, L.-M. Duan, C.-C. Joseph Wang, J. Freericks, and C. Monroe, Nat Commun **2**, 377 (2011).
[18] J. W. Britton, B. C. Sawyer, A. C. Keith, C.-C. J. Wang, J. K. Freericks, H. Uys, M. J. Biercuk, and J. J. Bollinger, Nature **484**, 489 (2012).
[19] R. Islam, C. Senko, W. C. Campbell, S. Korenblit, J. Smith, A. Lee, E. E. Edwards, C.-C. J. Wang, J. K. Freericks, and C. Monroe, Science **340**, 583 (2013).
[20] C. Schneider, D. Porras, and T. Schaetz, Reports on Progress in Physics **75**, 024401 (2012).
[21] J. Berges, S. Borsányi, and C. Wetterich, Physical Review Letters **93**, 142002 (2004).
[22] M. Kollar, F. A. Wolf, and M. Eckstein, Physical Review B **84**, 054304 (2011).
[23] R. Barnett, A. Polkovnikov, and M. Vengalattore, Physical Review A **84**, 023606 (2011).
[24] M. v. d. Worm, B. C. Sawyer, J. J. Bollinger, and Michael Kastner, arXiv:1209.3697 (2012).
[25] M. Heyl, A. Polkovnikov, and S. Kehrein, arXiv:1206.2505 (2012).
[26] K. Kim, M.-S. Chang, R. Islam, S. Korenblit, L.-M. Duan, and C. Monroe, Physical Review Letters **103**, 120502 (2009).
[27] M. Rigol, A. Muramatsu, and M. Olshanii, Physical Review A **74**, 053616 (2006).
[28] A. V. Ponomarev, S. Denisov, and P. Hänggi, Physical Review Letters **106**, 010405 (2011).
[29] C. Albanese, M. Christandl, N. Datta, and A. Ekert, Physical Review Letters **93**, 230502 (2004).
[30] N. Y. Yao, Z.-X. Gong, C. R. Laumann, S. D. Bennett, L.-M. Duan, M. D. Lukin, L. Jiang, and A. V. Gorshkov, Physical Review A **87**, 022306 (2013).
[31] S. Olmschenk, K. C. Younge, D. L. Moehring, D. N. Matsukevich, P. Maunz, and C. Monroe, Physical Review A **76**, 052314 (2007).